Multi-color light curves and orbital period research of eclipsing binary V1073 Cyg

RAA 2018 Vol. **18** No. **2**, 20(10pp) doi: 10.1088/1674–4527/18/2/20

http://www.raa-journal.org *http://iopscience.iop.org/raa*

***R**esearch in*
***A**stronomy and*
***A**strophysics*

Multi-color light curves and orbital period research of eclipsing binary V1073 Cyg

Xiao-Man Tian[1,2,3], Li-Ying Zhu[1,2,3], Sheng-Bang Qian[1,2,3], Lin-Jia Li[1,2,3] and Lin-Qiao Jiang[4]

[1] Yunnan Observatories, Chinese Academy of Sciences, Kunming 650216, China; *joie@ynao.ac.cn*
[2] Key Laboratory of the Structure and Evolution of Celestial Objects, Chinese Academy of Sciences, Kunming 650216, China
[3] University of Chinese Academy of Sciences, Beijing 100049, China
[4] School of Physics and Electronic Engineering, Sichuan University of Science & Engineering, Zigong 643000, China

Received 2017 June 28; accepted 2017 November 27

Abstract New multi-color BVR_cI_c photometric observations are presented for the W UMa type eclipsing binary V1073 Cyg. The multi-color light curve analysis with the Wilson-Devinney procedure yielded the absolute parameters of this system, showing that V1073 Cyg is a shallow contact binary system with a fill-out factor $f = 0.124(\pm0.011)$. We collected all available times of light minima spanning 119 yr, including CCD data to construct the $O-C$ curve, and performed detailed $O-C$ analysis. The $O-C$ diagram shows that the period change is complex. A long-term continuous decrease and a cyclic variation exist. The period is decreasing at a rate of $\dot{P} = -1.04(\pm0.18) \times 10^{-10}\,\mathrm{d\ cycle^{-1}}$and, with the period decrease, V1073 Cyg will evolve to the deep contact stage. The cyclic variation with a period of $P_3 = 82.7(\pm3.6)$ yr and an amplitude of $A = 0.028(\pm0.002)$ d may be explained by magnetic activity of one or both components or the light travel time effect caused by a distant third companion with $M_3(i' = 90^\circ) = 0.511\,M_\odot$.

Key words: stars: binaries: close — stars: binaries: eclipse — stars: binaries: individual (V1073 Cyg)

1 INTRODUCTION

V1073 Cyg (BD $+33^\circ$ 4252, HD 204038, HIP 105739, BV 342) is a W UMa type eclipsing binary. Strohmeier (1960) first recognized the variability of V1073 Cyg, then the photographic (pg) light curve was published in 1962 (Strohmeier 1962). Thus far, more photometric and spectrographic researches have been carried out for V1073 Cyg (such as Sezer 1993; Morris & Naftilan 2000; Yang & Liu 2000; Ekmekçi et al. 2012), and absolute parameters have been derived. Here is a brief introduction. The radial velocity curve was first reported by Fitzgerald (1964) and the mass ratio $q = 0.34$ was obtained. The latest mass ratio $q = 0.303(17)$ was presented by Pribulla et al. (2006) based on their radial-velocity curve. The fill-out factor has been reported many times, such as $f = 0.007$ and $f = 0.008$ (Kondo 1966; Leung & Schneider 1978; Ahn et al. 1992; Sezer 1993, 1994), $f = 0.19$ (Jafari et al. 2006) and $f = 0.20$ (Sezer 1996). The original classification of the spectral type of the primary star was A3 Vm (Fitzgerald 1964); some other spectral type classifications were also reported as F0n III-IV (Abt & Bidelman 1969), F0n V (Morgan et al. 1943) and F0V (Pribulla et al. 2006). Investigations about V1073 Cyg have confirmed that this system is a short-period contact eclipsing system with a period of $P = 0.7858506$ d (Pribulla et al. 2006).

The orbital period analysis has been undertaken by many authors. Aslan & Herczeg (1984) found that the period decreased by about 0.4 seconds in 1976 using 25 photoelectric (pe) and some pg epochs of minima since 1962. Then, Wolf & Diethelm (1992) conducted a new $O-C$ analysis by adding 16 pe times of light minima and identified a constant decrease. One year later, Sezer (1993) analyzed 29 pe data and reported that the period was decreasing by 3.12($\pm$0.17) seconds per century (i.e. $\dot{P} = -7.8 \times 10^{-10}\,\mathrm{d\ cycle^{-1}}$). Seventeen years ago, Morris & Naftilan (2000) pointed out that the period had

decreased by 0.795 ± 0.040 s around JD 2445000 in 1982, while Yang & Liu (2000) found that the period was decreasing at a rate of $\dot{P} = -8.8 \times 10^{-10}$ d cycle^{-1}from 1962 to 1998, using 111 data including 62 pe data in their analysis. By now, more high-precision eclipse times have been obtained, which are very useful for more precise period investigation.

According to the spectroscopic observation made by Fitzgerald (1964), the spectrum of the primary component shows that the primary component of V1073 Cyg is an Am star. V1073 Cyg has been listed in the catalog of Ap, HgMn and Am stars (Renson & Manfroid 2009) as a doubtful Am star. Almost all Am stars are A or F type stars with remarkably peculiar characteristics of element abundances, such as a rather weak Ca II, K line (Titus & Morgan 1940; Roman et al. 1948), underabundance of calcium and scandium, overabundances of iron-group elements and extreme enhancements of rare-earth elements (Conti 1970) compared to the same spectral type stars. Am stars rotate more slowly than normal A and F type stars, and the rotational velocities are always less than about $100\,\mathrm{km\,s^{-1}}$ (Abt & Moyd 1973); Am stars show a high binary proportion, which is more than 90% (Abt 1961, 1965; Hubrig et al. 2010). As the only known W UMa type binary among the 73 discovered eclipsing Am binaries (Renson & Manfroid 2009; Smalley et al. 2014), V1073 Cyg is very special because the rotational velocity of the primary component is about 160 $\mathrm{km\,s^{-1}}$ (Pribulla et al. 2006), which is much higher than the limiting rotational velocity of $100\,\mathrm{km\,s^{-1}}$ given by Abt & Moyd (1973). This makes it a challenge to interpret the cut-off of rotation velocity. So, both photometric and spectroscopic investigations of this target are very important.

In this study, we generated a new photometric solution for V1073 Cyg based on our new multi-color light curves and derived new absolute parameters. We also collected the times of minima for V1073 Cyg spanning 119 years and made a new exhaustive orbital period analysis.

2 OBSERVATION AND DATA REDUCTION

Light curve observations of V1073 Cyg were carried out with four filters on 2015 October 26, 27, 28 and 29 using the Andor DZ936 2K CCD (size: 2048×2048 pixel) photometric system attached to the 85 cm telescope (labeled as 'D80 cm') at Xinglong Station, which is administered by National Astronomical Observatories, Chinese Academy of Sciences (NAOC). Observations of minima light times were acquired on 2015 June 17 using 'D80 cm' and on 2015 September 28 using the Andor DW436 2K CCD camera mounted on the 60 cm reflecting telescope (labeled as 'D60 cm') managed by Yunnan Observatories in China (YNO). The images were processed with the PHOT package of IRAF in standard mode. Then, differential magnitudes were determined, by choosing BD+32 4152 as the comparison star and TYC 2707-276-1 as the check star. The relevant information is listed in Table 1 and the finding chart is shown in Figure 1.

Table 1 Information on V1073 Cyg, and the Comparison and Check Stars

	Variable (V) V1073 Cyg	Comparison (C) BD+32 4152	Check (Ch) TYC 2707–276–1
α_{2000}	$21^{\mathrm{h}}25^{\mathrm{m}}00.35766^{\mathrm{s}}$	$21^{\mathrm{h}}25^{\mathrm{m}}10.6007^{\mathrm{s}}$	$21^{\mathrm{h}}23^{\mathrm{m}}10.72^{\mathrm{s}}$
δ_{2000}	$+33^\circ41'14.9435''$	$+33^\circ34'09.306''$	$+33^\circ23'29.9''$
V (mag)	8.38	8.77	12.18

3 LIGHT CURVES AND ANALYSES

New multi-color curves of V1073 Cyg were obtained in this study. Photometric phases were calculated with the new linear ephemeris

$$\begin{aligned}\mathrm{MinI} &= 2457191.2159(0.0003)\\ &\quad +0.7858506^{\mathrm{d}} * E,\end{aligned} \tag{1}$$

in which 2457191.2159 is the new time of light minimum obtained by this study, $P = 0.7858506$ d was given by Pribulla et al. (2006), and E is the cycle number. The phased multi-color light curves are plotted in Figure 2 with different colors marking the observations from different days, and corresponding magnitude differences between the comparison star and the check star are shown in the bottom panel.

Absolute parameters of this system were derived from the light curve analysis with Mode 3 in the Wilson-Devinney (W-D) program (Wilson & Devinney 1971; Wilson 1979, 1990; Van Hamme & Wilson 2007; Wilson 2008; Wilson et al. 2010; Wilson 2012). In the solution process, we adopted $q = 0.303$ and F0V as the spectral type of the primary star (Pribulla et al. 2006). Then referring to table 15.7 (Calibration of MK spectral types) in the book named Allen's Astrophysical Quantities by Cox (2000), the temperature of the primary star (star 1 in Mode 3) should be $T_1 = 7300$ K; the convergent photometric solutions are derived and listed in Table 2. We tried to set the third light l_3 as a free parameter, but failed to obtain a convergent solution. Based on Kepler's Third Law and $(M_1 + M_2)\sin i^3 = 1.896(25)$ (Pribulla et al. 2006), the absolute parameters (M_1, M_2, R_1, R_2, a) can be derived and are listed in Table 2. The theoretical light curves are plotted in Figure 3, while the geometrical structure is shown in Figure 4.

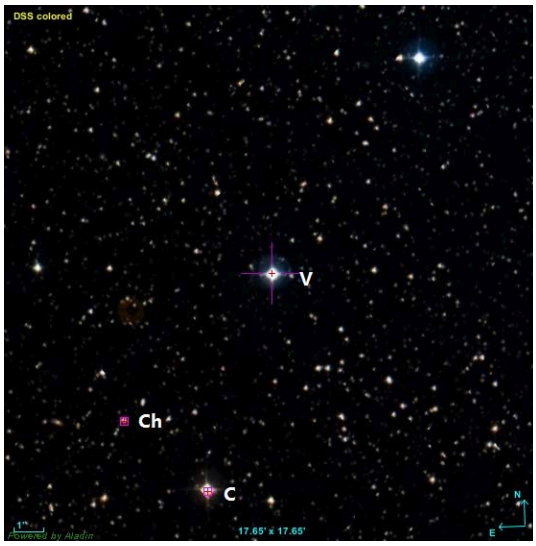

Fig. 1 Finding chart. 'V','C' and 'Ch' represent 'Variable star', 'Comparison star' and 'Check star', respectively.

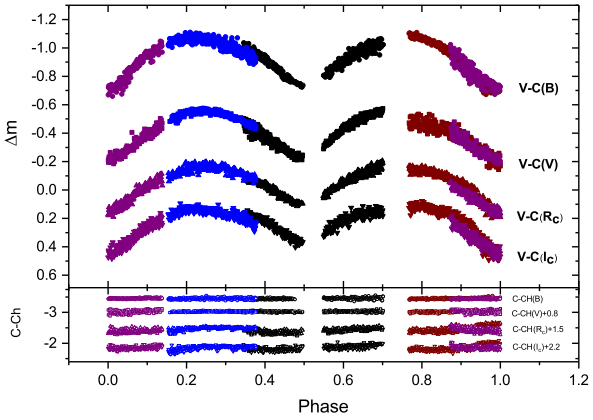

Fig. 2 The phased light curves of V1073 Cyg. *Circles*, *squares*, *triangles* and *down triangles* represent B, V, R_c and I_c band observation data respectively, and *open symbols* show the corresponding magnitude differences between the comparison star and the check star.

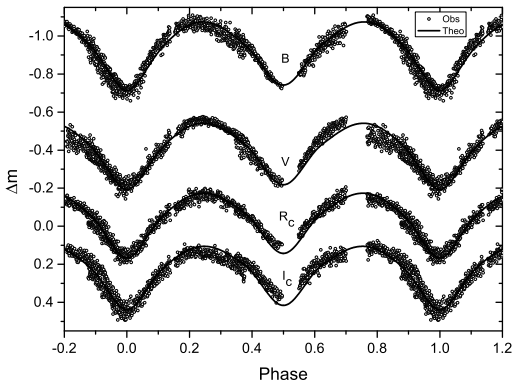

Fig. 3 The observed (*circles*) and theoretical light curves (*solid lines*) of V1073 Cyg.

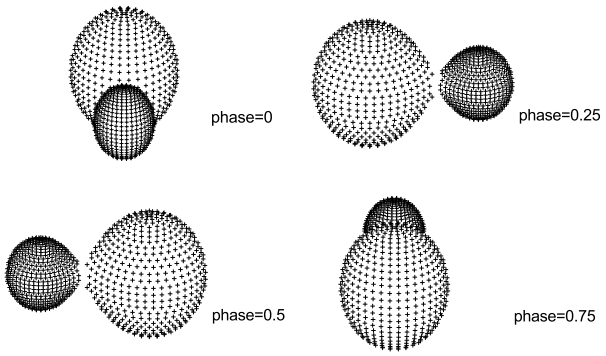

Fig. 4 Geometrical structure of V1073 Cyg at phases 0.0, 0.25, 0.5 and 0.75.

Table 2 Photometric Solutions of V1073 Cyg

Parameter	Value
Mode	3
$q(M_2/M_1)$	0.303(fixed)
M_1 $(M_\odot)$	1.810($\pm$0.004)
M_2 $(M_\odot)$	0.549($\pm$0.001)
R_1 $(R_\odot)$	2.545($\pm$0.008)
R_2 $(R_\odot)$	1.481($\pm$0.009)
a $(R_\odot)$	5.172($\pm$0.030)
i (°)	68.4($\pm$0.1)
T_1 (K)	7300
T_2 (K)	6609($\pm$18)
Ω_1	2.450($\pm$ 0.002)
$L_1/L_{\rm total}(B)$	0.832($\pm$0.002)
$L_1/L_{\rm total}(V)$	0.829($\pm$0.002)
$L_1/L_{\rm total}(R_c)$	0.804($\pm$0.002)
$L_1/L_{\rm total}(I_c)$	0.794($\pm$0.003)
$f(\rm fill-out)$	0.124($\pm$0.011)
r_1 (pole)	0.460($\pm$0.0005)
r_1 (side)	0.496($\pm$0.0006)
r_1 (back)	0.522($\pm$0.0008)
r_2 (pole)	0.267($\pm$0.0005)
r_2 (side)	0.279($\pm$0.0006)
r_2 (back)	0.315($\pm$0.0010)
$\sum(O-C)^2$	0.035

4 $O-C$ DIAGRAM ANALYSES

We collected 257 times of light minima from 1899 to 2017 and observed three times in 2015. All these 260 times of light minima are listed in Table 3. The time HJD 2447408.7690 that was observed by the spectrographic method was discarded because of its obvious deviation from the $O-C$ diagram, and all the others listed in Table 3 were used for the $O-C$ analysis. The $O-C$ values were determined by the observed (O) mid-eclipse times minus the calculated (C) times with the ephemeris (1). The corresponding $O-C$ diagram is shown in the upper panel of Figure 5 with dots, solid up triangles, pentagrams and open down triangles representing the 'CCD,' 'pe,' visual ('vis') and 'pg' data respectively.

The period decrease has been thoroughly discussed (Aslan & Herczeg 1984; Wolf & Diethelm 1992; Sezer 1993; Morris & Naftilan 2000; Yang & Liu 2000). We tried to fit the $O-C$ curve with a downward parabolic curve indicating period decrease, which is shown with a dashed line in the upper panel of Figure 5. The residuals $(O-C)_1$ from the parabolic fit are displayed in the middle panel, which also exhibits a cyclic oscillation indicating the existence of a cyclic variation. So, we combined the downward parabolic curve with a cyclic variation and tried to apply a good fit to the general trend of the $O-C$ curve. The combination curve is plotted in the upper panel of Figure 5 with a solid line. Taking the case (eccentric orbit) reported by Qian et al. (2015) into account, the following Equation (2) was used to describe the $O-C$ diagram

$$O-C \;=\; \Delta T_0 + \Delta P_0 \times E + 1/2\beta E^2 + \tau, \qquad (2)$$

where ΔT_0 is the the corresponding correction values for the epoch, ΔP_0 is the period in Equation (1) and β is the rate of linear change in the period (d cycle^{-1}). τ is the periodic variation caused by the light travel time effect (LTTE) (Irwin 1952), shown as $(O-C)_1$ in the middle panel of Figure 5,

$$\tau \;=\; A[(1-e^2)\frac{\sin(\nu+\omega)}{1+e\cos(\nu)} + e\sin(\omega)], \qquad (3)$$

$$\;=\; A[\sqrt{(1-e^2)}\sin E^*\cos\omega + \cos E^*\sin\omega], \qquad (4)$$

in which $A = a_{12}{}'\sin i'/c$ (d) is the projected semi-major axis and c is the speed of light; e, ν and ω are the eccentricity, true anomaly and longitude of the periastron passage respectively, and E^* is the eccentric anomaly. The Kepler equation leads to the relationship between the mean anomaly M and E^*

$$M \;=\; E^* - e\sin E^* = \frac{2\pi}{P_{\rm A}}(t-T). \qquad (5)$$

$P_{\rm A}$ is the anomalistic period, t is the time of light minimum and T is the time of periastron passage.

In our $O-C$ analysis, we adopt different weights for data with different precisions, i.e. a weight of 5 for CCD (ccd) and pe data, and a low weight of 1 for vis and pg data, which is the same as in Yang & Liu (2000). The combination of the change in continuum decrease and cyclic variation gives a good fit to the $O-C$ curve. All the fitting curves are displayed in Figure 5, with the solid line in the upper panel representing the combination of continuous decrease with a rate of $\dot{P} = -1.04(\pm0.18)\times10^{-10}\,{\rm d\ cycle^{-1}}$, and cyclic variation with a period of $P_3 = 82.7(\pm3.6)\,{\rm yr}$ and an amplitude of $A = 0.028(\pm0.002)\,{\rm d}$. In addition, the curve plotted in the middle panel is the cyclic variation $(O-C)_1$ after subtracting the continuous decrease, and the residuals are shown in the bottom panel. All results obtained from the above period analysis are listed in Table 4.

5 DISCUSSION AND CONCLUSIONS

V1073 Cyg is a short-period W UMa type eclipsing binary with a period of $P = 0.7858506\,{\rm d}$. Our new multicolor light curve analysis found that V1073 Cyg is a shallow contact binary, with a fill-out factor of f(*fill-out*) $= 0.124(\pm0.011)$, an orbital inclination angle of $i = 68.4(\pm2.9)^\circ$, and masses $M_1 = 1.810(\pm0.004)\,M_\odot$ and $M_2 = 0.549(\pm0.001)\,M_\odot$.

The $O-C$ analysis demonstrated that the orbital period of V1073 Cyg is simultaneously undergoing a continuous decrease and a cyclic variation. The period decrease rate $\dot{P} = -1.04(\pm0.18)\times10^{-10}\,{\rm d\ cycle^{-1}}$ is approximately consistent with $\dot{P} = -7.8\times10^{-10}\,{\rm d\ cycle^{-1}}$ of Sezer (1993) and $\dot{P} = -8.8\times10^{-10}\,{\rm d\ cycle^{-1}}$ of Yang & Liu (2000). More high-precision data (20 CCD data and more pe data) with the longest available time span (119 yr) were used in our analysis, so the results derived from our $O-C$ analysis should be more reliable. The long-term period changes could be explained by the combined effects of angular momentum loss and mass transfer between two components. With period decrease, V1073 Cyg will evolve from shallow contact stage to deep contact stage, then it will merge into a rapidly rotating single star, like V1309 Sco (Zhu et al. 2016). Long-term period variations (no matter decrease or increase) are very common for W UMa-type contact binaries, like V502 Oph (Derman & Demircan 1992), V417 Aql (Qian 2003), V1191 Cyg (Zhu et al. 2011), EP And (Liao et al. 2013), TY UMa (Samec et al. 2000), DD Ind (Samec et al. 2016) and so on.

The cyclic variation curve fits the $O-C$ diagram very well in Figure 5, and this is the first time that cyclic variation has been detected for V1073 Cyg. The period of the cyclic variation is $P_3 = 82.7(\pm3.6)\,{\rm yr}$ and the corresponding amplitude $A = 0.028(\pm0.002)\,{\rm d}$. There are two possible ways to interpret the cyclic variation, i.e. magnetic activity on one or both components (Applegate 1992), or the LTTE through the presence of a tertiary companion. In consideration of the short period and fast rotational velocity of about $160\,{\rm km\,s^{-1}}$, and the constitution of an F0V type primary component and a late type secondary component, it is probable that magnetic activity cycles (Applegate 1992; Lanza et al. 1998; Lanza & Rodonò 1999) in the two components may appear in V1073 Cyg. Using the equation given by Rovithis-Livaniou et al. (2000)

$$\Delta P = \sqrt{2[1-\cos(2\pi P/P_3)]}\times A, \tag{6}$$

where P_3 is the period of the cyclic oscillation, we can obtain the value of $\frac{\Delta P}{P}$. The variation of the momentum ΔQ causing such cyclic variation can be calculated with the following equation (Lanza & Rodonò 2002)

$$\frac{\Delta P}{P} = -9\frac{\Delta Q}{Ma^2}, \tag{7}$$

in which a is the separation between the two components. As $M_1 = 1.810\,M_\odot$, $M_2 = 0.549\,M_\odot$ and $a = 5.172\,R_\odot$, combining the above two equations, $\Delta Q_1 = 3.6\times10^{52}\,{\rm g\,cm^2}$ and $\Delta Q_2 = 1.7\times10^{52}\,{\rm g\,cm^2}$ can be obtained for the components, and the values of ΔQ_1 and ΔQ_2 are typical for close binaries, in which the ΔQ should be about $10^{51}\sim10^{52}\,{\rm g\,cm^2}$ (Lanza & Rodonò 1999); so the Applegate mechanism can be used to explain the cyclic period variation.

According to Liao & Qian (2010), LTTE due to the existence of a distant third companion may be a plausible reason for periodic variation of binaries. Such a third body would play an important role in the evolution of contact binaries. It would cause a periodic variation of period, and would also remove angular momentum from the system, leading to the orbital contraction process and promoting the evolution of such contact binaries (Tokovinin et al. 2006; Qian et al. 2013, 2014, 2017). Many binaries have been detected containing third body, such as GSC 4560–02157 (Han et al. 2016), TW Dra (Liao et al. 2016), KIC 7622486 (Zhang et al. 2017) and BO Lyn (Li et al. 2018).

In Table 2, $M_1 = 1.810(\pm0.122)\,M_\odot$ and $M_2 = 0.549(\pm0.037)\,M_\odot$, so the mass function of such a tertiary companion can be calculated with the equation

$$\begin{aligned} f(m) &= \frac{4\pi^2}{G{P_3}^2}\times({a_{12}}'\sin i')^3 \\ &= \frac{(M_3\sin i')^3}{(M_1+M_2+M_3)^2}. \end{aligned} \tag{8}$$

Table 3 The Times of Light Minima for V1073 Cyg

HJD (2400000+)	Error	Min.	Meth.	E	$(O-C)$ (d)	Ref.	HJD (2400000+)	Error	Min.	Meth.	E	$O-C$ (d)	Ref.
14801.8070		s	pg	–53940.5	–0.23464	[1]	23641.8050		s	pg	–42691.5	–0.27004	[1]
15601.7760		s	pg	–52922.5	–0.26155	[1]	23725.6350		p	pg	–42585	–0.13313	[1]
15694.5570		s	pg	–52804.5	–0.21092	[1]	23773.5110		p	pg	–42524	–0.19402	[1]
16029.6630		p	pg	–52378	–0.27021	[1]	23953.7910		s	pg	–42294.5	–0.26673	[1]
16033.6290		p	pg	–52373	–0.23346	[1]	23981.7990		p	pg	–42259	–0.15643	[1]
16330.6770		p	pg	–51995	–0.23698	[1]	24003.7020		p	pg	–42231	–0.25724	[1]
16413.5990		s	pg	–51889.5	–0.22222	[1]	24016.7300		s	pg	–42214.5	–0.19578	[1]
16990.8100		p	pg	–51155	–0.21849	[1]	24422.6000		p	pg	–41698	–0.21761	[1]
17021.7730		s	pg	–51115.5	–0.29659	[1]	24459.5240		p	pg	–41651	–0.22859	[1]
17145.5780		p	pg	–50958	–0.26306	[1]	24459.5730		p	pg	–41651	–0.17959	[1]
17432.8540		s	pg	–50592.5	–0.21545	[1]	24889.4780		p	pg	–41104	–0.13487	[1]
17458.7310		s	pg	–50559.5	–0.27152	[1]	25102.7440		s	pg	–40832.5	–0.22731	[1]
17497.6700		p	pg	–50510	–0.23213	[1]	25132.6900		s	pg	–40794.5	–0.14363	[1]
18283.4890		p	pg	–49510	–0.26373	[1]	25139.7130		s	pg	–40785.5	–0.19329	[1]
18683.4710		p	pg	–49001	–0.27968	[1]	25573.5570		s	pg	–40233.5	–0.13882	[1]
19238.7500		s	pg	–48294.5	–0.20413	[1]	25748.8230		s	pg	–40010.5	–0.11750	[1]
19308.6730		s	pg	–48205.5	–0.22183	[1]	25779.7880		p	pg	–39971	–0.19360	[1]
19668.6130		s	pg	–47747.5	–0.20141	[1]	25803.8140		s	pg	–39940.5	–0.13604	[1]
19948.8210		p	pg	–47391	–0.14915	[1]	25890.5740		p	pg	–39830	–0.21253	[1]
20005.7230		s	pg	–47318.5	–0.22132	[1]	25925.5250		s	pg	–39785.5	–0.23189	[1]
20012.7920		s	pg	–47309.5	–0.22497	[1]	26029.6670		p	pg	–39653	–0.21509	[2]
20046.6120		s	pg	–47266.5	–0.19655	[1]	26127.5070		s	pg	–39528.5	–0.21349	[2]
20407.6330:		p	pg	–46807	–0.27390	[1]	26352.2630		s	pg	–39242.5	–0.21076	[2]
20409.6140:		s	pg	–46804.5	–0.25752	[1]	26352.2750		s	pg	–39242.5	–0.19876	[2]
20667.7760		p	pg	–46476	–0.24745	[1]	26444.6100		p	pg	–39125	–0.20121	[2]
20763.6220:		p	pg	–46354	–0.27522	[1]	26547.5260		p	pg	–38994	–0.23164	[2]
20769.6100		s	pg	–46346.5	–0.18110	[1]	26547.5330		p	pg	–38994	–0.22464	[2]
20789.6380		p	pg	–46321	–0.19229	[1]	26547.5410		p	pg	–38994	–0.21664	[2]
21206.5220		s	pg	–45790.5	–0.20203	[1]	26547.5490		p	pg	–38994	–0.20864	[2]
21228.5130		s	pg	–45762.5	–0.21485	[1]	26547.5560		p	pg	–38994	–0.20164	[2]
21423.7610		p	pg	–45514	–0.25072	[1]	26547.5640		p	pg	–38994	–0.19364	[2]
21481.6310:		s	pg	–45440.5	–0.14074	[1]	26619.4290		s	pg	–38902.5	–0.23397	[2]
21488.6160		s	pg	–45431.5	–0.22840	[1]	26623.3410		s	pg	–38897.5	–0.25122	[2]
21542.5060		p	pg	–45363	–0.16916	[1]	26623.3620		s	pg	–38897.5	–0.23022	[2]
21544.4640		s	pg	–45360.5	–0.17579	[1]	26623.3840		s	pg	–38897.5	–0.20822	[2]
21731.7840:		p	pg	–45122	–0.28116	[1]	26623.4060		s	pg	–38897.5	–0.18622	[2]
21768.8060		p	pg	–45075	–0.19414	[1]	26624.5580		p	pg	–38896	–0.21299	[2]
21825.7460		s	pg	–45002.5	–0.22831	[1]	26675.2180		s	pg	–38831.5	–0.24036	[2]
21844.6320		s	pg	–44978.5	–0.20272	[1]	26711.4740		s	pg	–38785.5	–0.13349	[1]
21859.6030		s	pg	–44959.5	–0.16288	[1]	26861.5020		s	pg	–38594.5	–0.20295	[2]
21866.5970		s	pg	–44950.5	–0.24154	[1]	26913.7890		p	pg	–38528	–0.17502	[1]
22238.7070		p	pg	–44477	–0.23180	[1]	26915.3080		p	pg	–38526	–0.22772	[2]
22511.7940		s	pg	–44129.5	–0.22788	[1]	26926.7350		s	pg	–38511.5	–0.19555	[1]
22674.5270		s	pg	–43922.5	–0.16595	[1]	26929.5030		p	pg	–38508	–0.17803	[2]
22819.8350		s	pg	–43737.5	–0.24031	[1]	26979.3760		s	pg	–38444.5	–0.20654	[2]
22834.7770		s	pg	–43718.5	–0.22948	[1]	27000.2420		p	pg	–38418	–0.16558	[2]
22924.7720		p	pg	–43604	–0.21437	[1]	27002.5640		p	pg	–38415	–0.20113	[1]
23308.6560		s	pg	–43115.5	–0.21839	[1]	27026.5040		s	pg	–38384.5	–0.22958	[1]
23612.7870		s	pg	–42728.5	–0.21157	[1]	27036.3410		p	pg	–38372	–0.21571	[1]
23638.7110		s	pg	–42695.5	–0.22064	[1]	27241.8100		s	pg	–38110.5	–0.24664	[1]

[1] Strohmeier & Bauernfeind (1968). [2] Kondo (1966). [3] Wolf & Diethelm (1992). [4] Kruseman (1968). [5] Bonneville et al. (1975). [6] Dumitrescu & Dinescu (1976). [7] Braune et al. (1979). [8] Braune et al. (1981). [9] GEOS EB 13. [10] Aslan & Herczeg (1984). [11] BAV-M 34. [12] BAV-M 36. [13] Diethelm et al. (1983). [14] Scarfe et al. (1984). [15] Pohl et al. (1987). [16] BBSAG 80. [17] Keskin & Pohl (1989). [18] Ahn et al. (1992). [19] Wunder et al. (1992). [20] Muyesseroglu et al. (1996). [21] BAV-M 56. [22] B.R.N.O. data. [23] BAV-M 60. [24] BBSAG 99. [25] BBSAG 110. [26] Nelson (1998). [27] Rotse. [28] Derman & Kalci (2003). [29] Nelson (2003). [30] VSOLJ 42. [31] Brát et al. (2007). [32] Brát et al. (2008). [33] Yilmaz et al. (2009). [34] Hubscher et al. (2010). [35] Gokay et al. (2010). [36] Gokay et al. (2012). [37] Liakos & Niarchos (2011). [38] This study. [39] Hubscher (2016). [40] Juryšek et al. (2017).

Table 3 — *Continued.*

HJD (2400000+)	Error	Min.	Meth.	E	$O-C$ (d)	Ref.	HJD (2400000+)	Error	Min.	Meth.	E	$O-C$ (d)	Ref.
27267.8230		s	pg	–38077.5	–0.16671	[1]	34653.2960		s	pg	–28679.5	–0.11765	[2]
27272.4990		s	pg	–38071.5	–0.20581	[1]	36788.4650		s	pg	–25962.5	–0.10473	[2]
27313.3620		s	pg	–38019.5	–0.20705	[1]	36788.5100		s	pg	–25962.5	–0.05973	[2]
27333.4000		p	pg	–37994	–0.20824	[1]	36790.4600		p	pg	–25960	–0.07436	[2]
27354.5990		p	pg	–37967	–0.22720	[1]	36814.4180		s	pg	–25929.5	–0.08480	[2]
27632.8210		p	pg	–37613	–0.19631	[1]	36840.3440		s	pg	–25896.5	–0.09187	[2]
28027.6800		s	pg	–37110.5	–0.22724	[1]	36868.2610		p	pg	–25861	–0.07257	[2]
28032.7880		p	pg	–37104	–0.22727	[1]	37878.4707	0.0004	s	pe	–24575.5	–0.07381	[3]
28062.7270		p	pg	–37066	–0.15059	[1]	37928.3750		p	pe	–24512	–0.07102	[4]
28064.6470		s	pg	–37063.5	–0.19522	[1]	37935.4480		p	pe	–24503	–0.07068	[4]
28090.6030		s	pg	–37030.5	–0.17229	[1]	37939.3762	0.0005	p	pe	–24498	–0.07173	[3]
28126.3190		p	pg	–36985	–0.21249	[1]	37941.3401	0.0011	s	pe	–24495.5	–0.07246	[3]
28429.6470		p	pg	–36599	–0.22282	[1]	38327.5890		p	pe	–24004	–0.06823	[2]
28668.5600		p	pg	–36295	–0.20841	[1]	38353.5219		p	pe	–23971	–0.06930	[4]
28694.5070		p	pg	–36262	–0.19447	[1]	38662.3674		p	pe	–23578	–0.06309	[4]
28729.5040		s	pg	–36217.5	–0.16783	[1]	38669.4397		p	pe	–23569	–0.06344	[4]
28753.4870		p	pg	–36187	–0.15327	[1]	38672.5820		p	pe	–23565	–0.06454	[2]
28844.5480		p	pg	–36071	–0.25094	[1]	38692.6208		s	pe	–23539.5	–0.06493	[2]
29111.4510		s	pg	–35731.5	–0.14422	[1]	38707.5520		s	pe	–23520.5	–0.06489	[2]
29114.5400		s	pg	–35727.5	–0.19862	[2]	38731.5204		p	pe	–23490	–0.06494	[2]
29159.3880		s	pg	–35670.5	–0.14410	[2]	39040.3651		p	pe	–23097	–0.05952	[4]
29161.4550		p	pg	–35668	–0.04173	[2]	39077.3002		p	pe	–23050	–0.05940	[4]
29212.4940:		p	pg	–35603	–0.08302	[1]	39338.5946	0.0009	s	pe	–22717.5	–0.06033	[3]
29244.2330		s	pg	–35562.5	–0.17097	[2]	39340.5613	0.0014	p	pe	–22715	–0.05825	[3]
29465.4790		p	pg	–35281	–0.14191	[2]	39342.5232	0.0010	s	pe	–22712.5	–0.06098	[3]
29491.4230		p	pg	–35248	–0.13098	[2]	39355.4932	0.0016	p	pe	–22696	–0.05751	[3]
29516.5400		p	pg	–35216	–0.16120	[2]	42616.3970:		s	vis	–18546.5	–0.04078	[5]
29857.6350		p	pg	–34782	–0.12536	[1]	42660.4276		s	pe	–18490.5	–0.01781	[6]
30181.8000		s	pg	–34369.5	–0.12374	[1]	42662.3880		p	pe	–18488	–0.02204	[6]
30251.6300		s	pg	–34280.5	–0.23444	[1]	42671.4289		s	pe	–18476.5	–0.01842	[6]
30259.6160		s	pg	–34270.5	–0.10694	[1]	43005.4150		s	vis	–18051.5	–0.01883	[7]
30533.4650		p	pg	–33922	–0.12688	[1]	43012.5060		s	vis	–18042.5	–0.00048	[7]
30576.6840		p	pg	–33867	–0.12966	[1]	43014.4540		p	vis	–18040	–0.01711	[7]
30583.7570		p	pg	–33858	–0.12932	[1]	43016.4190		s	vis	–18037.5	–0.01673	[7]
30648.5350		s	pg	–33775.5	–0.18399	[1]	43715.4480		p	vis	–17148	–0.00184	[8]
30663.4950		s	pg	–33756.5	–0.15515	[1]	43722.5210		p	vis	–17139	–0.00150	[9]
30965.6670		p	pg	–33372	–0.14271	[1]	43731.5420		s	vis	–17127.5	–0.01778	[9]
30983.7290		p	pg	–33349	–0.15527	[1]	43744.5170		p	vis	–17111	–0.00932	[8]
31004.5510		s	pg	–33322.5	–0.15831	[1]	44506.7950		p	pe	–16141	–0.00640	[10]
31247.7890		p	pg	–33013	–0.14107	[1]	44783.4139		p	pe	–15789	–0.00691	[10]
31319.7130		s	pg	–32921.5	–0.12240	[1]	44790.4489		p	pe	–15780	–0.00356	[10]
31323.5970		s	pg	–32916.5	–0.16766	[1]	44816.4330		p	vis	–15747	0.00647	[11]
31328.7300		p	pg	–32910	–0.14269	[1]	45216.4400		p	pg	–15238	0.01551	[12]
31341.6860		s	pg	–32893.5	–0.15322	[1]	45275.3750		p	pe	–15163	0.01172	[13]
31673.7350		p	pg	–32471	–0.12610	[1]	45568.8845		s	pe	–14789.5	0.00602	[14]
32053.6710		s	pg	–31987.5	–0.14886	[1]	46291.4714	0.0010	p	pe	–13870	0.00329	[15]
32381.8010		p	pg	–31570	–0.11149	[1]	46614.4600		p	pe	–13459	0.00729	[16]
33575.5100		p	pg	–30051	–0.10955	[1]	47326.4385		p	pe	–12553	0.00515	[17]
34636.4150		p	pg	–28701	–0.10286	[2]	47348.4413		p	pe	–12525	0.00413	[17]
34651.3360		p	pg	–28682	–0.11302	[2]	47350.4067		s	pe	–12522.5	0.00491	[17]
47357.4820		s	pe	–12513.5	0.00755	[17]	48864.3487	0.0008	p	pe	–10596	0.00573	[20]
47377.5175		p	pe	–12488	0.00386	[17]	48865.5247	0.0013	s	pe	–10594.5	0.00295	[20]
47408.7690		p	sp	–12448	–0.17866	[18]	49236.4492	0.0014	s	pe	–10122.5	0.00597	[20]
47748.4413		p	pe	–12016	0.00618	[19]	50968.8568	0.0020	p	pe	–7918	0.00592	[26]
47761.4060	0.0010	s	pe	–11999.5	0.00434	[20]	51001.8627	0.0005	p	pe	–7876	0.00609	[26]
47763.3764	0.0008	p	pe	–11997	0.01012	[20]	51326.4150		p	ccd	–7463	0.00210	[27]
47776.3453	0.0009	s	pe	–11980.5	0.01248	[20]	52130.3446		p	pe	–6440	0.00653	[28]

Table 3 — *Continued.*

HJD (2400000+)	Error	Min.	Meth.	E	$O-C$ (d)	Ref.	HJD (2400000+)	Error	Min.	Meth.	E	$O-C$ (d)	Ref.
47822.3117		p	pe	–11922	0.00662	[21]	52144.4867		p	pe	–6422	0.00332	[28]
47822.3191		p	pe	–11922	0.01402	[21]	52172.3871		s	pe	–6386.5	0.00602	[28]
47840.3834		p	pe	–11899	0.00376	[21]	52569.6317		p	pe	–5881	0.00315	[29]
47840.3840		p	pe	–11899	0.00436	[21]	52874.1509		s	ccd	–5493.5	0.00524	[30]
48106.3953	0.0015	s	pe	–11560.5	0.00523	[20]	54317.3616	0.0020	p	ccd	–3657	0.00131	[31]
48106.4010	0.0080	s	pe	–11560.5	0.01093	[3]	54617.5533	0.0009	p	ccd	–3275	–0.00192	[32]
48115.4316		p	pe	–11549	0.00425	[19]	54697.3165	0.0002	s	ccd	–3173.5	–0.00255	[33]
48132.3293	0.0027	s	pe	–11527.5	0.00616	[20]	54698.4943	0.0002	p	ccd	–3172	–0.00353	[33]
48145.2951	0.0010	p	pe	–11511	0.00542	[20]	54720.5010	0.0004	p	ccd	–3144	–0.00065	[33]
48482.4214		p	pe	–11082	0.00182	[3]	55083.5635	0.0005	p	pe	–2682	–0.00112	[34]
48482.4268	0.0028	p	pe	–11082	0.00722	[19]	55089.4572	0.0008	s	ccd	–2674.5	–0.00130	[35]
48482.4272		p	pe	–11082	0.00762	[20]	55447.4114	0.0010	p	ccd	–2219	–0.00205	[36]
48484.3885	0.0054	s	pe	–11079.5	0.00429	[3]	55774.3275	0.0007	p	ccd	–1803	0.00020	[37]
48484.3966	0.0036	s	pe	–11079.5	0.01239	[20]	55777.4684	0.0008	p	ccd	–1799	–0.00230	[37]
48488.3169	0.0014	s	pe	–11074.5	0.00344	[20]	55779.4327	0.0002	s	ccd	–1796.5	–0.00263	[37]
48489.4935	0.0018	p	pe	–11073	0.00126	[20]	55793.5788	0.0003	s	ccd	–1778.5	–0.00184	[37]
48500.5030		p	pe	–11059	0.00885	[22]	55799.4728		p	ccd	–1771	–0.00172	[22]
48504.4299	0.0005	p	pe	–11054	0.00650	[3]	55873.3412		p	ccd	–1677	–0.00328	[22]
48532.3265	0.0007	s	pe	–11018.5	0.00540	[3]	57191.2159	0.0003	p	ccd	0	0.00000	[38]
48559.4382		p	pe	–10984	0.00526	[23]	57214.3977	0.0064	s	ccd	29.5	–0.00082	[39]
48559.4387		p	pe	–10984	0.00576	[23]	57294.1623	0.0005	p	ccd	131	0.00002	[38]
48598.3360		s	pe	–10934.5	0.00345	[24]	57324.0210	0.0006	p	ccd	169	–0.00123	[38]
48823.4853		p	pe	–10648	0.00656	[25]	57644.64990	0.0002	p	ccd	577	–0.00183	[40]

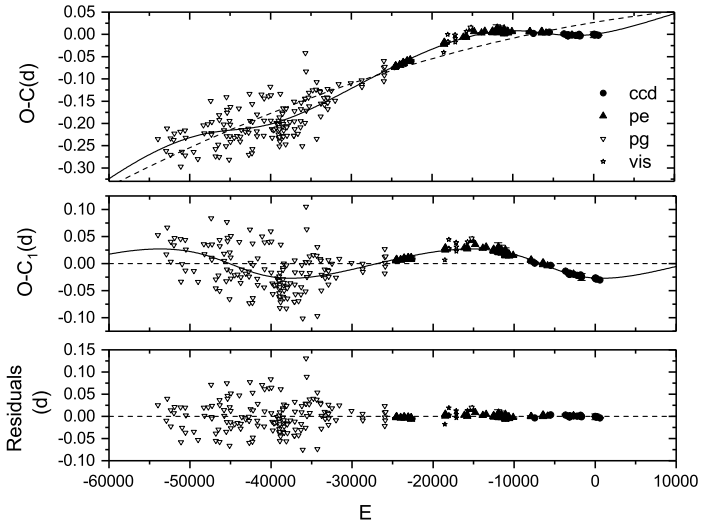

Fig. 5 $O-C$ diagram of V1073 Cyg. *Dots*, *solid up triangles*, *open down triangles* and *pentagrams* mark the CCD, pe, pg and vis data respectively. The *solid line* in the *upper panel* is the combination of the continuous decrease and the cyclic variation, while the *sine-like curve* in the *middle panel* represents the cyclic variation $(O-C)_1$ after subtracting the continuous decrease; the residuals are shown in the *bottom panel*.

In the formula, G is the gravitational constant and P_3 is the orbital period of the tertiary component. $a_{12}{}'\sin i' = 4.84(\pm0.34)\,(\mathrm{AU})$ leads to $f(m) = 0.017(\pm0.004)\,M_\odot$, and if $i' = 90°$, then $M_3 = 0.511\,M_\odot$ and $a_3 = 21.368$ AU can be calculated. This study is the first time the sign of the existence of a third body in V1073 Cyg has been detected. Our $O-C$ analysis shows that the mass of the third body is a little less than the mass of the second component, but we failed to fit the light curve with the third light. No third body has been identified from light curve analysis in previous researches, and the radial velocity curves (Fitzgerald 1964; Pribulla et al. 2006) did not show any evidence of a potential third body. One possible explanation is that the

Table 4 Orbital Parameters of V1073 Cyg from the $O-C$ Diagram Analysis

Parameter	Value
Revised epoch, ΔT_0 (d)	0.026834($\pm$0.004848)
Revised period, ΔP_0 (d)	3.0261848($\pm$0.4545760) $\times 10^{-6}$
Rate of the linear decrease, β (d cycle^{-1})	–1.04($\pm$0.18) $\times 10^{-10}$
Eccentricity, e_3	0.26($\pm$0.15)
Longitude of the periastron passage, $\omega_3(^\circ)$	197.9($\pm$25.3)
Time of periastron passage, T_3	2453082.8($\pm$ 2111.1)
Semi-amplitude, A (d)	0.028($\pm$0.002)
Orbital period, P_3 (yr)	82.7($\pm$3.6)
Orbital semi-major axis, $a_{12}{}' \sin i'$(AU)	4.84($\pm$0.34)
Mass function, $f(m)(M_\odot)$	0.017($\pm$0.004)
Mass, $M_3(i'=90^\circ)(M_\odot)$	0.511
Orbital radius, $a_3(i'=90^\circ)$ (AU)	22.368

third body may be a white dwarf. In fact, the mass of the third body is around the mass peak distribution for white dwarfs.

In our opinion, the LTTE will be more plausible than the magnetic activity mechanism for interpreting the cyclic variation. Because, compared with the magnetic cycles shown in solar-type single stars and close binaries (Maceroni et al. 1990; Bianchini 1990), the period of 82.7 yr accounting for cyclic variation in V1073 Cyg is much longer. The LTTE may cause a strict cyclic variation of period instead of a simple period oscillation, which can be verified by more new CCD times of light minima data.

As we have mentioned that V1073 Cyg is a special doubtful Am binary because of the fast rotation velocity, from our light curve and $O-C$ curve analysis, we know that V1073 Cyg is a shallow contact binary and the period is undergoing a long-term decrease. The mass transfer and loss occurring in this shallow contact binary will lead to the orbit shrinking. Because of the synchronous rotation, the components of V1073 Cyg will rotate faster, which makes V1073 Cyg more interesting.

Acknowledgements This work is partly supported by the National Natural Science Foundation of China (Nos. 11573063, 11325315 and U1631108), the Key Science Foundation of Yunnan Province (No. 2017FA001), Chinese Academy of Sciences "Light of West China" Program and the research fund of Sichuan University of Science and Engineering (Grant No. 2015RC42).

New CCD photometric observations of the system were obtained with the 85 cm telescope at Xinglong station of National Astronomical Observatories, Chinese Academy of Sciences and the 60 cm telescope administered by Yunnan Observatories.

References

Abt, H. A. 1961, ApJS, 6, 37
Abt, H. A. 1965, ApJS, 11, 429
Abt, H. A., & Bidelman, W. P. 1969, ApJ, 158, 1091
Abt, H. A., & Moyd, K. I. 1973, ApJ, 182, 809
Ahn, Y. S., Hill, G., & Khalesseh, B. 1992, A&A, 265, 597
Applegate, J. H. 1992, ApJ, 385, 621
Aslan, Z., & Herczeg, T. J. 1984, Information Bulletin on Variable Stars, 2478
Bianchini, A. 1990, AJ, 99, 1941
Bonneville, T., Chetanneau, A., Desprez, F., et al. 1975, Bulletin der Bedeckungsveraenderlichen-Beobachter der Schweizerischen Astronomischen Gesellschaft, 23, 1
Brát, L., Zejda, M., & Svoboda, P. 2007, Open European Journal on Variable Stars, 74, 1
Brát, L., Šmelcer, L., Kuèáková, H., et al. 2008, Open European Journal on Variable Stars, 94, 1
Braune, W., Huebscher, J., & Mundry, E. 1979, Astronomische Nachrichten, 300, 165
Braune, W., Huebscher, J., & Mundry, E. 1981, Astronomische Nachrichten, 302, 53
Conti, P. S. 1970, PASP, 82, 781
Cox, A. N. 2000, Allen's astrophysical quantities (New York: AIP Press; Springer)
Derman, E., & Demircan, O. 1992, AJ, 103, 1658
Derman, E., & Kalci, R. 2003, Information Bulletin on Variable Stars, 5439
Diethelm, R., Elias, D. P., Germann, R., et al. 1983, Bulletin der Bedeckungsveraenderlichen-Beobachter der Schweizerischen Astronomischen Gesellschaft, 64, 1
Dumitrescu, A., & Dinescu, R. 1976, Information Bulletin on Variable Stars, 1116
Ekmekçi, F., Elmaslı, A., Yılmaz, M., et al. 2012, New Astron., 17, 603
Fitzgerald, M. P. 1964, Publications of the David Dunlap Observatory, 2, 417
Gokay, G., Demircan, Y., Terzioglu, Z., et al. 2010,

Information Bulletin on Variable Stars, 5922
Gokay, G., Demircan, Y., Gursoytrak, H., et al. 2012, Information Bulletin on Variable Stars, 6039
Han, Z. T., Qian, S. B., Irina, V., et al. 2016, RAA (Research in Astronomy and Astrophysics), 16, 156
Hubrig, S., González, J., & Schöller, M. 2010, in Astronomical Society of the Pacific Conference Series, 435, Binaries - Key to Comprehension of the Universe, eds. A. Prša, & M. Zejda, 257
Hubscher, J., Lehmann, P. B., Monninger, G., Steinbach, H.-M., & Walter, F. 2010, Information Bulletin on Variable Stars, 5941
Hubscher, J. 2016, Information Bulletin on Variable Stars, 6157
Irwin, J. B. 1952, ApJ, 116, 211
Jafari, M., Khalesseh, B., & Pazhouhesh, R. 2006, Ap&SS, 306, 29
Juryšek, J., Hoňková, K., Šmelcer, L., et al. 2017, Open European Journal on Variable Stars, 179, 1
Keskin, V., & Pohl, E. 1989, Information Bulletin on Variable Stars, 3355
Kondo, Y. 1966, AJ, 71, 54
Kruseman, P. 1968, Bulletin of the Astronomical Institutes of the Netherlands Supplement Series, 2, 377
Lanza, A. F., Rodono, M., & Rosner, R. 1998, MNRAS, 296, 893
Lanza, A. F., & Rodonò, M. 1999, A&A, 349, 887
Lanza, A. F., & Rodonò, M. 2002, Astronomische Nachrichten, 323, 424
Leung, K.-C., & Schneider, D. P. 1978, ApJ, 222, 917
Liakos, A., & Niarchos, P. 2011, Information Bulletin on Variable Stars, 6005
Liao, W.-P., & Qian, S.-B. 2010, MNRAS, 405, 1930
Liao, W.-P., Qian, S.-B., Li, K., et al. 2013, AJ, 146, 79
Liao, W.-P., Qian, S. B., Zejda, M., et al. 2016, RAA (Research in Astronomy and Astrophysics), 16, 94
Li, L. J., Qian, S. B., Zhang, J., et al. 2018, RAA (Research in Astronomy and Astrophysics), 18, 11
Maceroni, C., Bianchini, A., Rodono, M., van't Veer, F., & Vio, R. 1990, A&A, 237, 395
Morgan, W. W., Keenan, P. C., & Kellman, E. 1943, An Atlas of Stellar Spectra, with an Outline of Spectral Classification (Chicago: The University of Chicago Press)
Morris, S. L., & Naftilan, S. A. 2000, PASP, 112, 852
Muyesseroglu, Z., Gurol, B., & Selam, S. O. 1996, Information Bulletin on Variable Stars, 4380
Nelson, R. H. 1998, Information Bulletin on Variable Stars, 4621
Nelson, R. H. 2003, Information Bulletin on Variable Stars, 5371
Pohl, E., Akan, M. C., Ibanoglu, C., Sezer, C., & Gudur, N. 1987, Information Bulletin on Variable Stars, 3078
Pribulla, T., Rucinski, S. M., Lu, W., et al. 2006, AJ, 132, 769
Qian, S. 2003, A&A, 400, 649
Qian, S.-B., Liu, N.-P., Li, K., et al. 2013, ApJS, 209, 13
Qian, S.-B., Zhou, X., Zola, S., et al. 2014, AJ, 148, 79
Qian, S. B., Han, Z. T., Fernández Lajús, E., et al. 2015, ApJS, 221, 17
Qian, S.-B., He, J.-J., Zhang, J., et al. 2017, RAA (Research in Astronomy and Astrophysics), 17, 087
Renson, P., & Manfroid, J. 2009, A&A, 498, 961
Roman, N. G., Morgan, W. W., & Eggen, O. J. 1948, ApJ, 107, 107
Rovithis-Livaniou, H., Kranidiotis, A. N., Rovithis, P., & Athanassiades, G. 2000, A&A, 354, 904
Samec, R. G., Stoddard, M. L., & Faulkner, D. R. 2000, in Bulletin of the American Astronomical Society, 32, American Astronomical Society Meeting Abstracts #196, 745
Samec, R. G., Norris, C. L., Van Hamme, W., Faulkner, D. R., & Hill, R. L. 2016, AJ, 152, 219
Scarfe, C. D., Forbes, D. W., Delaney, P. A., & Gagne, J. 1984, Information Bulletin on Variable Stars, 2545
Sezer, C. 1993, Ap&SS, 208, 15
Sezer, C. 1994, Ap&SS, 215, 153
Sezer, C. 1996, Ap&SS, 245, 89
Smalley, B., Southworth, J., Pintado, O. I., et al. 2014, A&A, 564, A69
Strohmeier, W. 1960, in Veränderlichen-Colloquium Bamberg, Nr. 27, 1959, 1
Strohmeier, W. 1962, Information Bulletin on Variable Stars, 9
Strohmeier, W., & Bauernfeind, H. 1968, Bamberg Veroeffentlichungen der Remeis-Sternwarte, 7, 72
Titus, J., & Morgan, W. W. 1940, ApJ, 92, 256
Tokovinin, A., Thomas, S., Sterzik, M., & Udry, S. 2006, A&A, 450, 681
Van Hamme, W., & Wilson, R. E. 2007, ApJ, 661, 1129
Wilson, R. E. 1979, ApJ, 234, 1054
Wilson, R. E. 1990, ApJ, 356, 613
Wilson, R. E. 2008, ApJ, 672, 575
Wilson, R. E. 2012, AJ, 144, 73
Wilson, R. E., & Devinney, E. J. 1971, ApJ, 166, 605
Wilson, R. E., Van Hamme, W., & Terrell, D. 2010, ApJ, 723, 1469
Wolf, M., & Diethelm, R. 1992, Acta Astronomica, 42, 363
Wunder, E., Wieck, M., Kilinc, B., et al. 1992, Information Bulletin on Variable Stars, 3760
Yang, Y., & Liu, Q. 2000, Ap&SS, 274, 799
Yilmaz, M., Basturk, O., Alan, N., et al. 2009, Information Bulletin on Variable Stars, 5887
Zhang, J., Qian, S. B., & He, J. D., 2017, RAA (Research in Astronomy and Astrophysics), 17, 22
Zhu, L. Y., Qian, S. B., Soonthornthum, B., He, J. J., & Liu, L. 2011, AJ, 142, 124
Zhu, L.-Y., Zhao, E.-G., & Zhou, X. 2016, RAA (Research in Astronomy and Astrophysics), 16, 68